Annals of Biology **42** (2) : 179-184, 2026 **http://agribioj.com** **Impact Score : 0.32 (Scopus)**

Sustainable Green Synthesis of Zinc Oxide Nanoparticles from *Citrus sinensis* Peel Extract for Enhanced Antibacterial Activity

MAYANK RAJ, VIKAS KUMAR, CHARU BANSAL, AKASH SHARMA, VIVEK RAWAT[1], ZEENAT MADAN[2], SUSHIL KUMAR UPADHYAY, RAJ SINGH, DEEPAK YADAV[3] AND MANOJ SINGH*

Department of Bio-Sciences and Technology, MMEC, Maharishi Markandeshwar (Deemed to be University), Mullana, Ambala-133 207 (Haryana), India
**(e-mail: manoj.singh@mmumullana.org; Mobile: 87070 11151)*

(Received: January 2, 2026; Accepted: February 8, 2026)

ABSTRACT

Orange (*Citrus sinensis*) is a common fruit crop widely distributed worldwide with the peel of its fruits representing about 50% of fruit mass. In the current study, orange peel was employed to mediate the synthesis of zinc oxide nanoparticles (ZnO-NPs) in a low-cost green approach. This study involved the synthesis of zinc oxide nanoparticles (ZnO-NPs) through an environmentally friendly method, utilizing orange fruit peel aqueous extract both as a stabilizer and a biological reducing agent, utilizing zinc nitrate hexahydrate as the zinc precursor. This approach minimized the reliance on large quantities of chemicals and removal of hazardous substances from the fabrication process, enhancing the antibacterial properties of the nanoparticles. In UV-visible spectroscopy, a typical Zn^{2+} surface plasmon resonance band was found at 338 nm, confirming the formation of ZnO-NPs. HR-TEM confirmed that the particles were homogenous and spherical, ranging between 40 to 100 nm. The Fourier-Transform Infrared (FTIR) spectra revealed information about the extract's functional groups, which helped instabilizing ZnO-NPs. The strong and wide peak at 2359/cm was observed in the plant extract. The participation of the hydroxyl group (-OH) present in the extract's compounds reduced of zinc ions. The antimicrobial efficacy of the synthesized ZnO nanoparticles was assessed against gram positive and negative bacteria, *S. aureus*, *E. coli* and *P. aeruginosa, B. subtilis*, utilizing the well diffusion method on media favourable for bacterial proliferation. The synthesized nanoparticles demonstrated significant bactericidal properties, successfully suppressing bacterial proliferation and creating noticeable zones of inhibition.

Key words: Antibacterial activity, characterization, green synthesis, ZnO-NPs, zone of inhibition

INTRODUCTION

Over the last 10 years, the field of nanotechnology has experienced remarkable growth, propelled by its applications across various domains including medicine, chemistry and biotechnology. This advancement has opened up a plethora of opportunities in nanoscience, particularly evident in areas such as drug delivery, optoelectronics, nanomedicine and biosensing, among others. One of the most fascinating characteristics of nano-sized particles is their remarkable surface-to-volume ratio (Adhikari *et al*., 2024). This distinctive characteristic makes nanoparticles considerably more reactive than their bulk equivalents, due to the presence of a large surface area that facilitates reactions. Consequently, nanoparticles exhibit distinct properties when compared to their bulk counterparts (Bayda *et al*., 2019). The creation of these nanoparticles is accomplished using physical, chemical, or biological methods. Methods such as hydrothermal and sol-gel synthesis, laser ablation, microwave-assisted combustion and lithography, which fall under physical and chemical categories, require advanced equipment, proficient operators, significant energy resources and complex instrumentation. The methods in question present health risks as they frequently produce toxic by products during the synthesis process (Devatha and Thalla, 2018, Nocedo-Mena and

[1]Department of Chemistry, Government PG College, Thalisain Pauri Garhwal-246285 (Uttarakhand), India.
[2]Department of Zoology, Sanatan Dharma College, Ambala Cantt-133001 (Haryana), India.
[3]Department of Zoology, Miranda House (University of Delhi), New Delhi-110007, India.

Kharissova, 2024). The green synthesis approach has recently garnered significant attention. The nanoparticles are both cost-effective and environmentally-friendly, with the added benefit of being biodegradable. This approach is notable for being a budget-friendly option, devoid of harmful chemicals that may pose health risks, while also offering remarkable antimicrobial benefits (Parajuli *et al*., 2025). The environmentally-friendly approach to nanoparticle synthesis involves the use of various plant parts, bacteria, fungi and yeast, or their active products, serving as reducing and stabilizing agents.

ZnO has been recognized as one of the safest metal oxides by the U. S. Food and Drug Administration, noted for its anti-inflammatory and anticancer properties (Idris *et al*., 2025). Their adaptability and distinctive characteristics position them as leaders in the realm of nanotechnology, applicable across multiple disciplines. In this study, ZnO nanoparticles were synthesized using an aqueous extract of *Citrus sinensis* (orange) fruit peel as a stabilizing and capping agent, in conjunction with zinc nitrate hexahydrate as the zinc precursor. While there are studies that synthesize ZnO nanoparticles using orange peel extract, there is a lack of additional literature detailing the antibacterial properties and the environmentally-friendly synthesis of ZnO nanoparticles utilizing the *C. sinensis* plant (Gupta *et al*., 2025).

MATERIALS AND METHODS

The fruit of *C. sinensis* was purchased from a shop located nearby to the Maharishi Markandeshwar (Deemed to be University) Campus in Mullana. The peels were thoroughly cleaned three times with double distilled water then shade-dried in a dust-free environment for one week at room temperature before being cut to the suitable size. Zinc nitrate was acquired from Sigma-Aldrich (Bangalore, India). A 0.01M zinc solution was made using 1.317 g of zinc nitrate hexahydrate dissolved in 600 ml of distilled water. The solvent utilized in this experiment was refined using double distillation. To prepare the extracts, the orange fruit peel was washed, dried and then meticulously peeled as thinly as possible before undergoing further drying. The desiccated peels were pulverized into a fine powder. Subsequently, 1 g of the powder was deposited into various glass containers, each containing 50 ml of deionized water, and swirled for 3 h. After maceration, each mixture was subjected to a water bath at 60°C for 60 min. The combination was ultimately filtered using Whatman Filter Paper No. 1. The solution was preserved at 4 °C and utilized to produce zinc oxide nanoparticles (Luque-Alcaraz *et al*., 2025). Upon completion of the reaction, the crude nanoparticle solution required purification to exclude unreacted metallic salts and residual plant extract materials. The colloidal solution was transferred into sterile centrifuge tubes and centrifuged at high speed (e.g. 8,000 to 15,000 rpm for 15 min). This compelled the nanoparticles to aggregate toward the bottom, resulting in the formation of a pellet. The characteristic of synthesized ZnO-NPs was investigated by different characterization techniques. The bioreduction of $Zn(NO_3)_2$ in aqueous solution was observed with mixed plant extracts studies by using ultraviolet-visible near-infrared (UV-Vis-NIR) spectrophotometer (UV-2600, Shimadzu, Japan) ranging 200-700 nm. A high resolution transmission electron microscope (HRTEM) (JSM-7610F, Japan) was used to study the surface morphology of ZnO-NPs. Highly pure KBr powder was mixed with 1% (w/w) samples and then pressed into pellets to identify the bioactive functional group of ZnO-NPs by Fourier transform infrared spectroscopy (FTIR, PerkinElmer, USA) recorded within 4000-350/cm. The antibacterial activity of zinc oxide nanoparticles was assessed using the agar wells diffusion method, and the resultant zone of inhibition was measured. The antibacterial efficacy of the zinc oxide nanoparticle was evaluated against gram positive and negative bacteria *S. aureus, E. coli* and *P. aeruginosa, B. subtilis* using well diffusion method on MHA plates. The suspension of ZnO nanoparticles at along with its drug conjugates (10 µl) was placed in well diffusion method. The sample was incubated at 37°C for 24 h, and the zone of inhibition (ZOI) was measured with a ruler (Singh *et al*., 2022).

RESULTS AND DISCUSSION

The formation of zinc oxide nanoparticles was primarily identified by colour change. Visually *C. sinensis* fruit peel extract

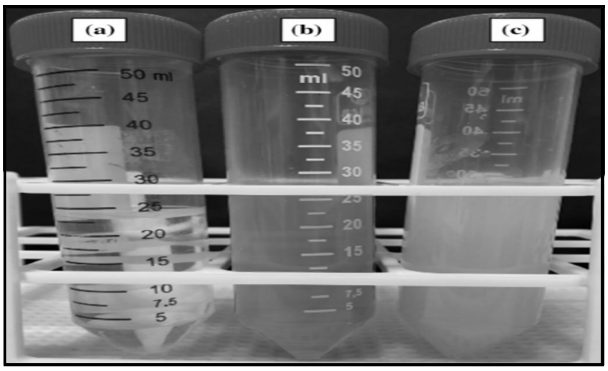

Fig. 1. Preliminary synthesis: (a) white colour of $Zn(NO_3)_2$, (b) yellow colour from aqueous fruit peel extract of *Citrus sinensis* and (c) dark brown colour change indicating the formation of zinc oxide nanoparticles.

was mixed with 0.01 M zinc nitrate hexahydrate solution showing a colour change from colour less to light yellow within 90 min then the colour changed from light yellow to brown and finally it turned to dark brown after 6 h at 80°C (Fig. 1). The colour intensity increased with time of incubation as well as the yellow coloured solution converted to dark brown within 5 h which may be due to the increased concentration of nanoparticles and the surface plasmon resonance in the aqueous solution (Biswas *et al*., 2024). Finally, no further colour change of the solution was observed after 24 h.

UV-Vis spectroscopy is an effective, reliable, sensitive and selective technique employed for the first identification of various types of nanoparticles. Furthermore, calibration is unnecessary for assessing the particle characteristics of the colloidal suspension (Yusuf-Salihu *et al*., 2025). Fig. 2 illustrates the UV-Vis absorption spectra of zinc oxide nanoparticles (ZnO-NPs) solution mediated by *C. sinensis* fruit peel extract, within the wavelength range of 200-700 nm. The baseline data were obtained using deionized water, also referred to as the sample blank in this analysis. The coloured samples were diluted with deionized water and placed in a quartz cell for UV spectroscopy, where absorption peaks were identified in the ultraviolet range of around 300-400 nm. The absorption peaks were identified at various time intervals of $Zn(NO_3)_2$ salt. The highest absorption peak (a.u 1.2) was seen at 7 h of incubation at 320 nm. The free electron between the conduction band and the valence band oscillates, producing a spectrum of

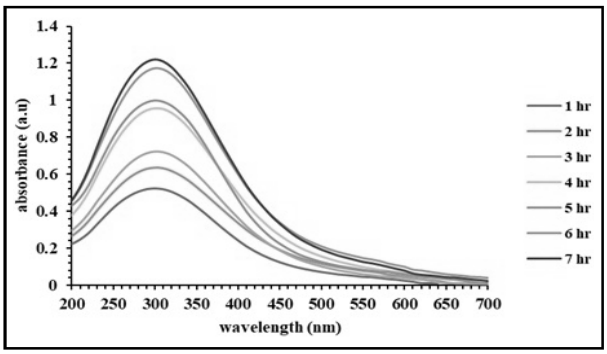

Fig. 2. Absorbance spectra of ZnO-NPs prepared using aqueous fruit peel extract.

absorption peaks due to the mass oscillation of the electrons in zinc oxide nanoparticles resonating with the optical wave at surface plasmon resonance (SPR) (Ghasemi *et al*., 2025). The primary factors influencing the absorption of ZnO-NPs are particle sizes and the surrounding chemical and electrical insulation (Subathra and Vellaisamy, 2024).

The biofunctionalized zinc oxide nanoparticles synthesized at 1 mM salt concentration at 80°C were characterized for particle size distribution. The maximum quantity and maximum amplitude recorded illuminated the dimensions and size distribution of zinc oxide nanoparticles. The determined particle size distribution by intensity was seen within the 10-120 nm range (Fig. 3). The average particle size was approximately 49.63 nm, with some particles exhibiting sizes ranging from 10 to 120 nm. The polydispersity index (PDI) was 20.7.

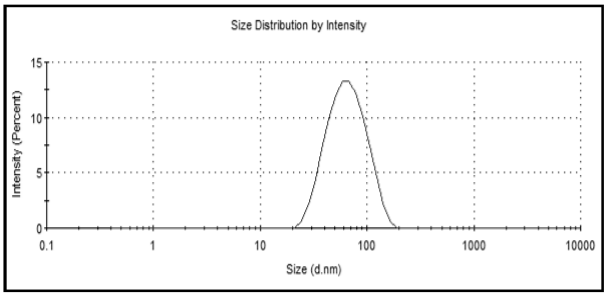

Fig. 3. Size distribution pattern of ZnO-NPs using DLS technique.

The shape of ZnO-NPs was examined using HR-TEM. Fig. 4 depicts a combination of plates (spherical and hexagonal) and spheres. Representative TEM pictures indicated that the size distribution of ZnO-NPs ranged from 60 to 100 nm. The high-resolution TEM revealed distinct lattice fringes on the surfaces of the particles.

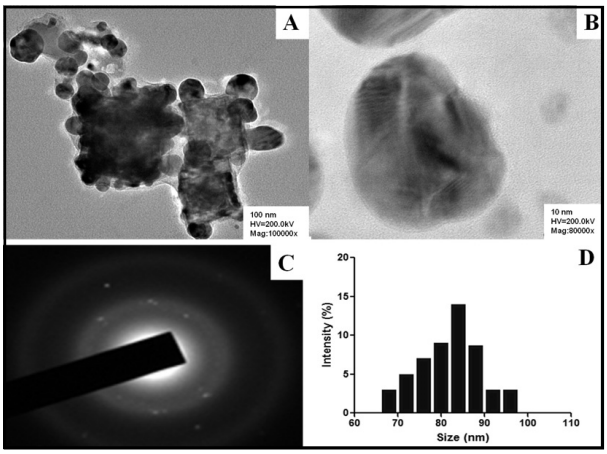

Fig. 4. (A and B) Transmission electron microscopy (TEM) images, (C) SAED images, and (D) histogram distribution plot of zinc oxide nanoparticles.

FTIR analysis was used for the functional group characterization from the peel extract of *C. sinensis* and the synthesized zinc oxide nanoparticles at 80°C (Fig. 5A and B). The absorbance bands were observed in the region of 500-4500 cm. The synthesis of ZnO-NPs showed stronger intense peak at 2359/cm, 2365/cm, 2176/cm, 2036/cm, 1947/cm and 1638/cm (Fig. 5 B). The FTIR spectra of the peel extract of *C. sinensis* after bio reduction showed some significant changes. There was an intense broad peak at 2359/cm which was attributed to the O-H stretching modes of vibration in hydroxyl functional group in alcohols and N-H stretching vibrations in amides and amines (Farjam *et al*., 2025). The intense peak at 2365/cm corresponded to C-H stretching vibration modes in the hydrocarbon chains. The band corresponding to the stretching vibrations of the carbonyl functional group in ketones, aldehydes and carboxylic acids were found to be at 2176/cm. The band at 2036/cm can be assigned to N=C=S stretching vibrations in aromatic compounds. The band at 1947/cm can be assigned to C-H bending. The band at 1638/cm can be assigned to C=C stretching vibration in alkenes. The observed peaks were mainly attributed due to presence of some secondary metabolites like flavonoids, triterpenes, tannins, steroids and saponins excessively present in fruit pulp extract as also suggested by other researchers (Rani *et al*., 2024; Ayub *et al*., 2025).

This study evaluated the antibacterial efficacy of *C. sinensis* extract and synthesized ZnO nanoparticles against four bacterial species. The zone of inhibition for Amoxicillin (10 µl) formulated zinc oxide nanoparticles for *S. aureus* was more significant than that for Ampicillin (10 µl) nanocolloids. Whereas, the zone of inhibition for both nanoformulated drugs against *E. coli* (amox. ~3.6 mmand amp. ~3 mm), *S. aureus* (amox.~3.9 mm and amp.~2.9 mm), *P. aeruginosa* (amox.~2.8 mm and amp.~3.8 mm) and *B. substilis* (amoxy.~3.1 mm and amp.~3.2 mm) were highly significant than its pure form (Figs. 6 and 7). Furthermore, the mechanism underlying the action of zinc oxide nanoparticles on bacterial membranes has been elucidated based on the composition of the cell wall. Gram-negative organisms are more susceptible due to their easier permeability. The attachment of metal nanoparticles and drug formulations to bacterial cells induces structural changes in the cell membrane and obstructs transport channels (Sharma *et al*., 2024). The inhibitory mechanism likely involves the impairment of genetic material replication and the immobilization of specific cellular proteins and

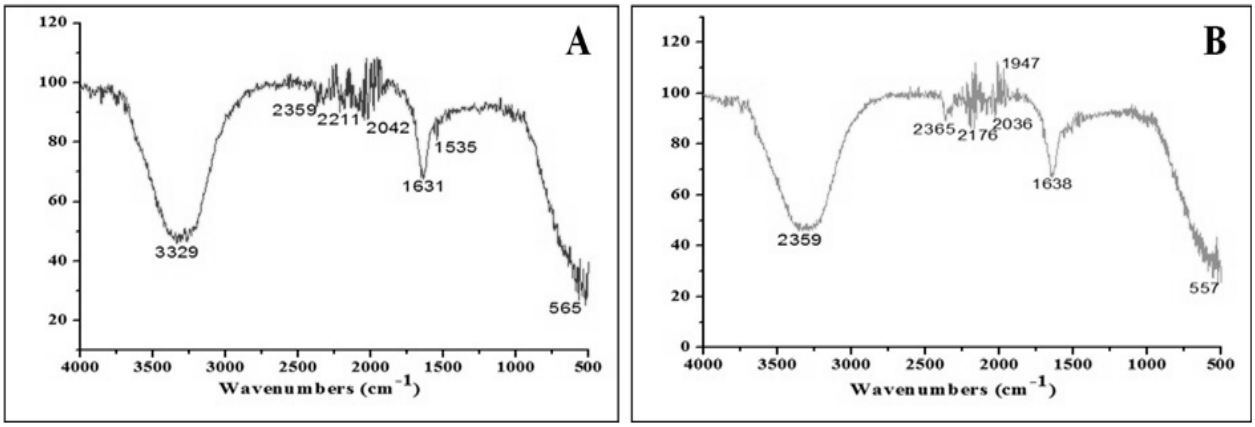

Fig. 5. FTIR spectra (A) *Citrus sinesis* fruit peel extract and (B) aqueous peel extract of ZnO-NPs.

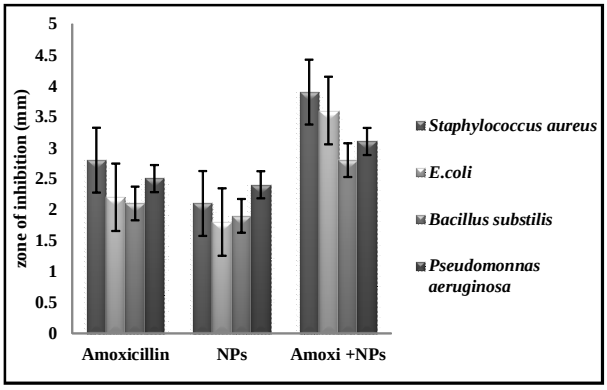

Fig. 6. Histogram of zone of inhibition for amoxicillin drug mixed with ZnO-NPs against the test bacteria.

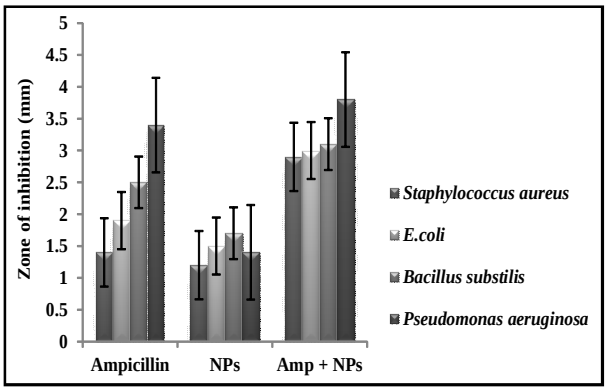

Fig. 7. Histogram of zone of inhibition for ampicillin drug mixed with ZnO-NPs against the test bacteria.

enzymes crucial for ATP synthesis. The antibacterial activity of ZnO nanoparticles mostly relies on their size and morphology, with smaller, spherical particles exhibiting more toxicity. Numerous investigations have indicated that spherical nanoparticles, measuring approximately 10-120 nm, serve as effective antibacterial agents plant-derived ZnO nanoparticles can infiltrate bacterial cells, interacting with proteins, enzymes and DNA, resulting in cell death (Singh *et al*., 2021).

CONCLUSION

The observed reduction in conductivity during the synthesis process offers initial evidence for the reduction of zinc ions and the possible creation of ZnO nanoparticles. UV-Vis spectral analysis verified that the peak absorption occurred within the 300–400 nm range, characteristic of ZnO nanoparticles. An elevation in the concentration of the reducing agent led to a reduction in the band gap of ZnO nanoparticles and a displacement of the absorption maxima toward longer wavelengths. FTIR examination revealed distinctive peaks at 2359, 2365, 2176, 2036, 1947 and 1638/cm thereby affirming the synthesis of ZnO nanoparticles. The TEM investigation validated the dimensions and shape of the nanoparticles. Examination showed significant antibacterial activities of the synthesized AgNPs solution. The zone of inhibition in homogeneously showed a promising result against Gram-negative bacteria (*E. coli, P. aeruginusa*) and Gram-positive bacteria (*S. aureus, B. subtilis*) in combination with antibiotics. Moreover, Amoxicillin ZnO-NPs and Ampicillin –ZnO-NPs also significantly reduced the host cells cytotoxicity. The exact mechanism of action of these nanoparticles is not precisely understood and it is the subject of future studies along with testing their potential *in vivo*.

ACKNOWLEDGEMENTS

The authors are also thankful to the Department of Bio-Sciences and Technology, M.M.D.U., Mullana.

REFERENCES

Adhikari, K., Timilsina, A. and Chen, H. (2024). The effects of size and surface-coating of CuO-nanoparticles on extractable Cu and enzyme activities in soil. *Soil Environ. Health* **2**: 100065. *https://doi.org/10.1016/j.seh.2024.100065.*

Ayub, A., Anjum, K. M., Akram, W., Liaqat, H., Xue, S., Habib, A. and Majeed, M. B. B. (2025). Silver nanoparticles: Green synthesis and eco-friendly synthetic approaches, characterization and biological applications. *https://doi.org/10.5772/intechopen.1012460.*

Bayda, S., Adeel, M., Tuccinardi, T., Cordani, M. and Rizzolio, F. (2019). The history of nanoscience and nanotechnology: From chemical-physical applications to nanomedicine. *Molecules* **25**: 112. *https://doi.org/10.3390/molecules25010112.*

Biswas, K., Ahamed, Z., Dutta, T., Mallick, B., Khuda-Bukhsh, A. R., Biswas, J. K. and Mandal, S. K. (2024). Green synthesis of silver nanoparticles from waste leaves of tea (*Camellia sinensis*) and their catalytic potential for degradation of azo dyes. *J. Mol. Str.* **1318**: 139448. *https://doi.org/10.1016/j.molstruc.2024.139448.*

Devatha, C. P. and Thalla, A. K. (2018). Green synthesis of nanomaterials. In: *Synthesis of Inorganic Nanomaterials* pp. 169-184. Woodhead Publishing. *https://doi.org/10.1016/B978-0-08-101975-7.00007-5.*

Farjam, H., Mohammadi, S., Larijani, K. and Hosseini, S. (2025). Green synthesis gold nanoparticle from *Rosa damascena*: Antioxidant, antimicrobial and cytotoxic activities on nerve cells and inhibitory effects on Parkinson's disease. *Art. Cells, Nanomedicine Biotech.* **53**: 543-556. *https://doi.org/10.1080/21691401.2025.2583019.*

Ghasemi, M., Govahi, M. and Litkohi, H. R. (2025). Green synthesis of silver nanoparticles (AgNPs) and chitosan-coated silver nanoparticles (CS-AgNPs) using Ferulagummosa Boiss. gum extract: A green nano drug for potential applications in medicine. *Int. J. Biol. Macromolecules* **291**: 138619. *https://doi.org/10.1016/j.ijbiomac.2024.138619.*

Gupta, S., Choudhary, D. K. and Sundaram, S. (2025). Green synthesis and characterization of silver nanoparticles using *Citrus sinensis* (Orange peel) extract and their antidiabetic, antioxidant, antimicrobial and anticancer activity. *Waste Biomass Valorization* **16**: 1101-1114. *https://doi.org/10.1007/s12649-024-02782-z.*

Idris, D. S., Roy, A., Malik, A., Khan, A. A., Sharma, K. and Roy, A. (2025). Green synthesis of silver oxide-nickel oxide bimetallic nanoparticles using peels of *Citrus sinensis* and their application. *J. Inorg. Organometallic Polymers Mat.* **35**: 594-606. *https://doi.org/10.1007/s10904-024-03316-9.*

Luque-Alcaraz, A. G., Maldonado-Arriola, J. A., Hernández-Abril, P. A., Álvarez-Ramos, M. E. and Hernández-Téllez, C. N. (2025). Zein nanoparticles loaded with *Vitis vinifera* L. grape pomace extract: Synthesis and characterization. *Nanomaterials* **15**: 539. *https://doi.org/10.3390/nano15070539.*

Nocedo-Mena, D. and Kharissova, O. V. (2024). Nanoparticles derived from the Cissus genus and their antibacterial potential. *Environ. Nanotech. Monit. Man.* **22**: 100967. *https://doi.org/10.1016/j.enmm.2024.100967.*

Parajuli, K., Khanal, L. N., Gc, G., Koju, S., Bhujel, S., Khadka, D., Sharma, M. L., Pant, B. and Poudel, B. R. (2025). Lentil-husk-mediated green synthesis of silver nanoparticles: Characterization and antibacterial activity. *Chem Eng.* **9**: 17. *https://doi.org/10.3390/chemengineering9010017.*

Rani, N., Yadav, S., Mushtaq, A., Rani, S., Saini, M., Rawat, S. and Maity, D. (2024). *Azadirachta indica* peel extract-mediated synthesis of ZnO nanoparticles for antimicrobial, supercapacitor and photocatalytic applications. *Chem. Papers* **78**: 3687-3704. *https://doi.org/10.1007/s11696-024-03340-6.*

Sharma, V., Sharma, J. K., Kansay, V., Dutta, A., Raj, M., Singh, M. and Bera, M. K. (2024). Green synthesis, characterization and drug-loaded iron oxide nanoparticles derived from *Nerium oleander* flower extract as a nanocarrier for in vitro antibacterial efficacy. *Nano Express* **5**: 015014. *https://doi.org/10.1088/2632-959X/ad2997.*

Singh, M., Renu, V. K., Upadhyay, S. K., Singh, R., Yadav, M., Seema, S. K. and Manikandan, S. (2021). Biomimetic synthesis of silver nanoparticles from aqueous extract of *Saraca indica* and its profound antibacterial activity. *Biointerface Res. Appl. Chem.* **11**: 8110-8120. *https://doi.org/10.33263/BRIAC111.81108120.*

Singh, M., Thakur, V., Kumar, V., Raj, M., Gupta, S., Devi, N., Upadhyay, S. K., Macho, M., Banerjee, A., Ewe, D. and Saurav, K. (2022). Silver nanoparticles and their mechanistic insight for chronic wound healing: Review on recent progress. *Molecules* **27**: 5587. *https://doi.org/10.3390/molecules27175587.*

Subathra, M. and Vellaisamy, M. (2024). Green synthesis and characterization of cerium oxide nanoparticles using Piper Betle Leaves. *Rasayan J. Chem.* **17**: *https://doi.org/10.31788/RJC.2024.1718325.*

Yusuf-Salihu, B. O., Abdulmumini, S. A., Bajepade, T. T., Durosinmi, H. A., Kazeem, M. O., Ajayi, V. A. and Lateef, A. (2025). Novel green synthesis of silver nanoparticles from empty fruit bunch waste: Biomedical applications and mechanistic insights. *Next Nano.* **7**: 100136. *https:doi.org/10.1016/j.nxnano.2025.100136.*